Interconversion Pathways of the Protonated β-Ionone Schiff Base: An Ab Initio Molecular Dynamics Study

FRANK TERSTEGEN,[1] EMILY A. CARTER,[2] VOLKER BUSS[1]

[1] *Institut für Physikalische und Theoretische Chemie, Gerhard-Mercator-Universität, D-46047 Duisburg, Germany*

[2] *Department of Chemistry and Biochemistry, Box 951569, University of California at Los Angeles, Los Angeles, California 90095-1569*

Received 16 September 1998; revised 13 October 1998

ABSTRACT: Ab initio molecular dynamics at the RHF/3-21G level have been performed to study interconversion pathways (bond rotation and ring inversion) of the protonated β-ionone Schiff base. Starting with different stationary points on the Born–Oppenheimer potential energy surface, the trajectories are followed for 2100 fs. A perfunctory analysis of the reaction pathways reveals a dynamical behavior in agreement with classical expectations. © 1999 John Wiley & Sons, Inc. Int J Quant Chem 75: 141–145, 1999

Key words: ab initio molecular dynamics; bacteriorhodopsin; rhodopsin; protonated β-ionone Schiff base

Introduction

Retinal is the chromophore of several photochromic proteins. In rhodopsin, which is the photoreceptor for dim-light vision in the vertebrate retina, the visual cascade is initiated by photochemical isomerization of the 11-cis isomer of retinal Schiff base to the all-trans form. In bacteriorhodopsin, which is a membrane protein of the salt-loving *Halobacterium salinarium*, light energy is transformed into a proton gradient in a cyclic process which starts by photochemical isomerization of all-trans to 13-cis-retinal Schiff base. In both proteins the chromophore is covalently linked as a protonated Schiff base to the protein backbone [1, 2].

Quantum-mechanical calculations of the chromophore and on chromophore model systems, employing both force-field and semiempirical methods [3] and ab initio theories [4–7], have helped

Correspondence to: V. Buss.
Contract grant sponsor: U.S. Office of Naval Research.

© 1999 John Wiley & Sons, Inc.
CCC 0020-7608 / 99 / 030141-05

considerably in getting more insights into the molecular structures involved. For an improved description, more elaborate techniques are in use to model the time evolution of the system [8–11].

Computational Methods

Ab initio molecular dynamics (AIMD) has been developed as a nonempirical method for studying the dynamical behavior of molecular systems on a microscopic level [12]. The principle is straightforward: quantum-mechanically derived forces are used to integrate Newton's equations of motion for the nuclei. The calculations to be discussed below are based on an approach in which the wave function is reoptimized at each time step to ensure that the system remains on the Born–Oppenheimer potential energy surface [13].

The Gaussian94 program package [14] was used for the ab initio part of the calculations. The structures of all stationary points were fully optimized at the RHF/3-21G level and characterized through their second derivatives. Also, the SCF energy and the forces were calculated at this level for every point along the trajectory. For the molecular dynamics (MD) simulations a classical microcanonical molecular dynamics code was used, in which the integration of the classical equation of motion is done by the velocity Verlet integrator scheme [15].

In this algorithm the positions and the velocities at the same time point are given by

$$\mathbf{r}_i(t+\Delta t) = \mathbf{r}_i(t) + \mathbf{v}_i(t)\,\Delta t + \frac{\Delta t^2}{2m_i}\mathbf{F}_i(t)$$

$$\mathbf{v}_i(t+\Delta t) = \mathbf{v}_i(t) + \frac{\Delta t}{2m_i}[\mathbf{F}_i(t) + \mathbf{F}_i(t+\Delta t)]$$

where $\mathbf{r}_i(t)$, $\mathbf{r}_i(t+\Delta t)$ refer to the position, m_i to the mass, $\mathbf{v}_i(t)$, $\mathbf{v}_i(t+\Delta t)$ to the velocity, and $\mathbf{F}_i(t)$, $\mathbf{F}_i(t+\Delta t)$ to the force on the ith atom at times t and $t+\Delta t$.

By "freezing" the high-frequency stretching modes (fast vibrational modes) involving hydrogen, one can make the integration time steps longer. In the framework of the velocity Verlet scheme, the RATTLE algorithm of Andersen [16] is used to apply these constraints, which result in the following equations for the positions and velocities:

$$\mathbf{r}_i(t+\Delta t) = \mathbf{r}_i(t) + \mathbf{v}_i(t)\Delta t + \frac{\Delta t^2}{2m_i}\left[\mathbf{F}_i(t) - 2\sum_j \lambda_{ij}(t)\mathbf{r}_{ij}(t)\right]$$

$$\mathbf{v}_i(t+\Delta t) = \mathbf{v}_i(t) + \frac{\Delta t}{2m_i}\left[\mathbf{F}_i(t) - 2\sum_j \lambda_{ij}(t)\mathbf{r}_{ij}(t) + \mathbf{F}_i(t+\Delta t) - 2\sum_j \lambda'_{ij}(t+\Delta t)\mathbf{r}_{ij}(t+\Delta t)\right]$$

with $\mathbf{r}_{ij}(t) = \mathbf{r}_i(t) - \mathbf{r}_j(t)$ and λ_{ij} and λ'_{ij} the time-dependent Lagrange multipliers associated with the constraints on nuclear positions and velocities, respectively. In all MD calculations the energy is conserved, i.e., the total energy remains constant during the simulation.

In our calculations the starting geometries were stationary points generated on the Born–Oppenheimer potential energy surface. Forces were generated by slightly distorting the equilibrium geometry; velocities for all atoms were zeroed at the beginning of the MD run. Constraints were applied to all bonds with hydrogen atoms, i.e., C—H and N—H, with bond lengths fixed to their equilibrium values. One trajectory was run from each of four different stationary points. The time step in all simulations was 30 au (ca. 0.7 fs), and 3000 steps were calculated in each run.

Results and Discussion

The quantum-mechanical part of the simulation is the limiting factor for the size of the molecules which can be treated by AIMD. The retinals with more than 20 heavy atoms are still beyond this limit. β-Ionone, a molecule with a total of 36 atoms, shares with retinal all structural features of the cyclohexene end group, viz. the conjugation with a conjugated double-bond system and the substitution with three methyl groups (Scheme 1).

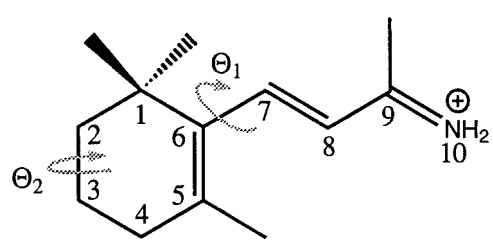

SCHEME 1

As a model for the retinal chromophore we have studied recently the cyclohexene ring inversion and the C6—C7 rotation in β-ionone derivatives [5]. As a result, on a two-dimensional subspace of the Born–Oppenheimer potential energy surface we have located all stationary points, i.e., minima, first-order saddle points (transition states) and second- and third-order saddle points (Fig. 1). In this figure, the coordinates Θ_1 and Θ_2 are the dihedral angles ∠C5C6C7C8 and ∠C1C2C3C4 and correspond, respectively, to rotation about the C6—C7 bond (horizontally) and inversion of the cyclohexene ring (vertically). The stationary points are drawn in perspective and in a bird's-eye view to give an impression of the subspace. Their RHF/3-21G energies together with the exact values of Θ_1 and Θ_2 are collected in Table I.

To briefly characterize the stationary points, (a) and (b) are the two highly twisted 6-s-cis conformers with the cyclohexene ring in either of the

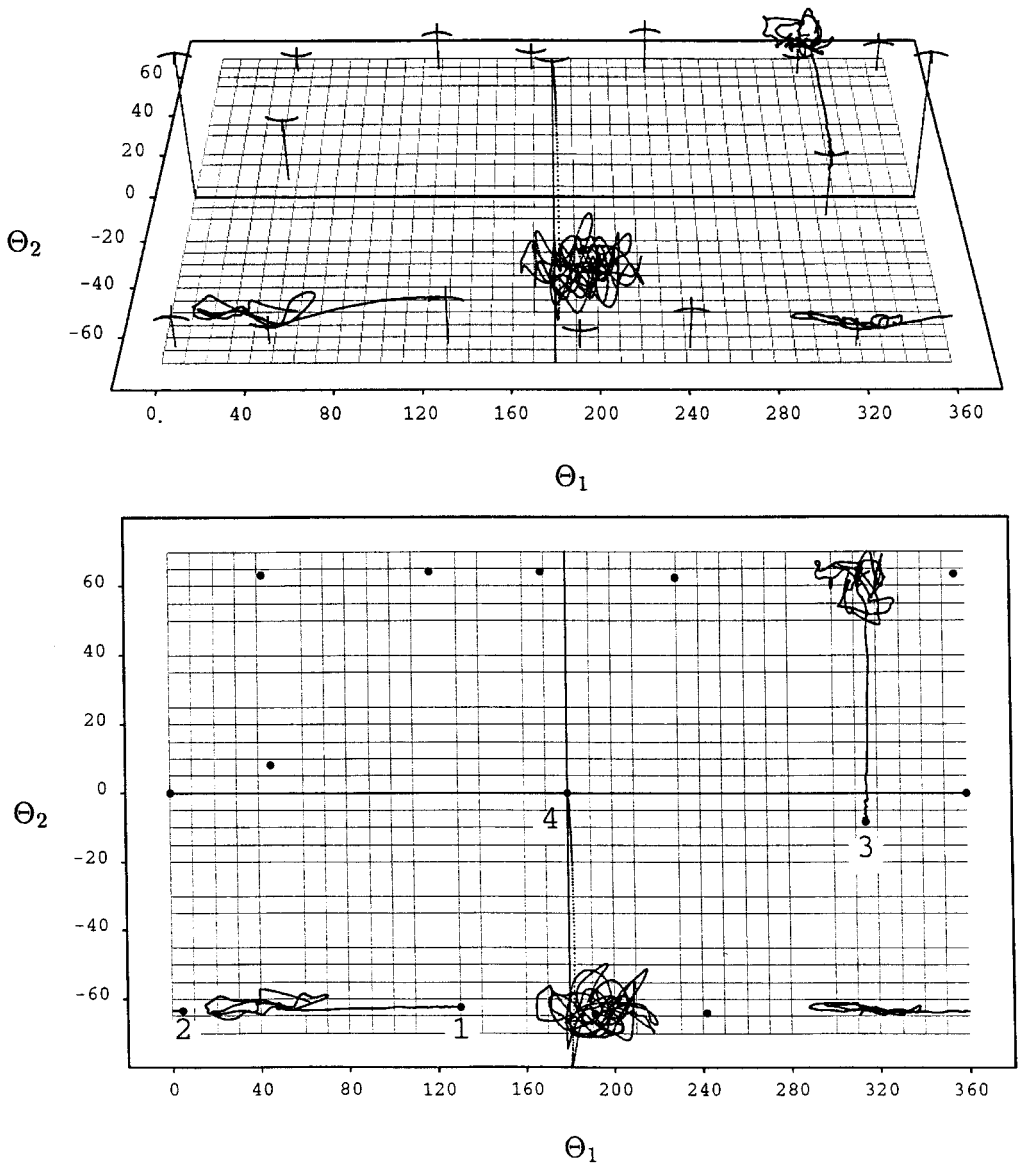

FIGURE 1. Perspective (top) and bird's-eye view (bottom) of RHF / 3-21G calculated trajectories. Stationary points (black dots) on the potential energy map are fully characterized; the potential functions are schematic and should help only in identifying the structures as minima, transition states or higher order saddle points. Note that the trajectory initiated at transition state 2 wraps around on the figure due to the periodicity of Θ_1.

TABLE I
Geometries (selected dihedral angles, degrees), total (Hartree) and relative energies (kcal / mol), and number of imaginary frequencies of RHF / 3-21G optimized structures.

Θ_2	Θ_1	Reference to text / Fig. 1	RHF / 3-21G	ΔE	i
−62.2	47.8	(a)	−556.2351856	0	0
−63.2	318.0	(b)	−556.2351489	0.02	0
−64.2	191.3	(c)	−556.2349423	0.15	0
−62.4	130.2	(d) / 1	−556.2292957	3.70	1
−64.1	241.9	(e)	−556.2305835	2.89	1
−63.4	4.8	(f) / 2	−556.2323711	1.77	1
−8.3	314.5	(g) / 3	−556.2263452	5.55	1
0.0	180.0	(h) / 4	−556.2116059	14.80	2
0.0	0.0	(i)	−556.2098439	15.90	3

possible half-chair conformations; (c) is the corresponding 6-s-trans conformer; (d) and (e) are the transition states for interconversion between the 6-s-trans conformer and either of the two 6-s-cis conformers (a) or (b) via bond rotation about C6—C7, (f) is the corresponding transition state for direct interconversion of (a) and (b); (g) represents the transition state for interconverting (b) and the mirror image of (a) via ring inversion; (h) is a planar (symmetry C_s) saddle point of second order for the two cyclohexene conformations and (i) likewise, with an additional imaginary frequency for C6—C7 bond rotation, respectively.

Molecular dynamics simulations were started from four different stationary points, viz., the first-order saddle points 1, 2, and 3 and the second-order saddle point 4; the trajectories show how the two dihedrals develop during the simulations.

As a typical run consider the calculation which starts at 1, which is the transition state for the interconversion between the 6-s-cis and the 6-s-trans conformation. The run was started by twisting Θ_1 by 2° from its stationary value of 130.2°. The trajectory first runs smoothly in the direction of the 6-s-cis minimum, picking up kinetic energy along the way. As a consequence the molecule cannot relax into the minimum-energy structure. Instead, it passes through the minimum, picking up potential energy and increasingly distributing energy into other internal coordinates. At some point along its path the conversion is complete (after ca. 983 fs), and the molecule returns, the repetition of this process giving rise to a Lissajous-figure-type reaction pathway of the trajectory.

The energy difference between the transition state 1 and the 6-s-cis minimum is 3.7 kcal/mol. The corresponding difference between the saddle point 4 and the 6-s-trans minimum is much higher, ca. 14.7 kcal/mol. The MD run starting at 4 reflects this difference directly: The system relaxes very fast (note the dotted trajectory, which indicates resolved single geometries), the first inflection point is reached after only 173 fs, and the number of oscillations performed in the identical time span is significantly higher, as can be seen in Figure 1. The center of these Lissajous figures is the trans minimum-energy structure. Despite its high energy the system does not pass over the transition states flanking this 6-s-trans minimum because the energy is distributed among several internal degrees of freedom.

Conclusions

We have shown that Born–Oppenheimer AIMD calculations using atom-centered bases on systems the size of β-ionone (36 atoms!) are feasible; the computational resources needed are moderate (each MD run took about 1 week on four nodes of an SPP 2000). Coupled with the calculation of other observables such as charge fluctuations or excited-state properties such as UV or CD-spectral data, this ab initio MD method appears to be a promising alternative to classical empirical potential MD for complex biomolecule potential energy surfaces.

ACKNOWLEDGMENT

One of us (E.A.C.) acknowledges the U.S. Office of Naval Research for partial support of this work. Part of this research was done in connection with the Graduiertenkolleg ''Structure and dynamics of heterogeneous systems.'' The calculations were performed at the Rechenzentrum Duisburg and at the Regionales Rechenzentrum Köln.

References

1. Birge, R. R.; Einterz, C. M.; Knapp, H. M.; Murray, L. P. Biophys J 1988, 53, 367; Birge, R. R.; Biochim Biophys Acta 1990, 1016, 293; Hargrave, P. A.; McDowell, J. H. Int Rev Cytol 1992, 137B, 49; Nathans, J. Biochemistry 1992, 31, 4923.

2. Photophysics and Photochemistry of Retinal Proteins; Special Issue; Isr J Chem 1995, 35.
3. Birge, R. R.; Hubbard, L. M. J. J Am Chem Soc 1980, 102, 2195; Tavan, P.; Schulten, K.; Oesterhelt, D. Biophys J 1985, 47, 415; Liu, S. H.; Mirzadegan, T. J Am Chem Soc 1988, 110, 8617; Ippel, J. H.; Spijker-Assink, M. B.; Groesbeek, M.; van der Stten, R.; Altona, C.; Lugtenburg, J. Recl Trav Chim Pays Bas 1994, 113, 99; Dehu, C.; Hendrickx, E.; Clays, K.; Persoons, A.; Bredas, J. L. Synth Metals 1995, 71, 1697; Xu, D.; Sheves, M.; Schulten, K. Biophys J 1995, 69, 2745.
4. Poirier, R. A.; Yadav, A.; Surjan, P. R. Can J Chem 1987, 65, 892; Poirier, R. A.; Yadav, A.; Surjan, P. R. J Mol Struct (Theochem) 1988, 167, 321; Poirier, R. A.; Yadav, A. Chem Phys Lett 1989, 156, 122; Yadav, A.; Poirier, R. A. Chem Phys Lett 1989, 164, 68; Yadav, A.; Poirier, R. A. J Photochem Photobiol 1991, A58, 191; Toto, J. L; Toto, T. T.; de Melo, C. P.; Robins, K. A. J Chem Phys 1994, 101, 3945; Froese, R. D. J.; Komaromi, I.; Byun, K. S.; Morokuma, K. Chem Phys Lett 1997, 272, 335.
5. Terstegen, F.; Buss, V. Chem Phys 1997, 225, 163.
6. Terstegen, F.; Buss, V. J Mol Struct (Theochem) 1996, 369, 53; Terstegen, F.; Buss, V. Chem Lett 1996, 449; Terstegen, F.; Buss, V. J Mol Struct (Theochem) 1998, 430, 209.
7. Buss, V.; Kolster, K.; Terstegen, F.; Vahrenhorst, R. Angew Chem Int Ed Engl 1998, 37, 1893.
8. Tallent, J. R.; Hyde, E. W.; Findsen, L. A.; Fox, G. C.; Birge, R. R. J Am Chem Soc 1992, 114, 1581.
9. Bifone, A.; de Groot, H. J. M.; Buda, F. Chem Phys Lett 1996, 248, 165; Buda, F.; de Groot, H. J. M.; Bifone, A. Phys Rev Lett 1996, 77, 4474; Bifone, A.; de Groot, H. J. M.; Buda, F. Pure Appl Chem 1997, 69, 2105; Bifone, A.; de Groot, H. J. M.; Buda, F. J Phys Chem 1997, B101, 2954.
10. Schulten, K.; Humphrey, W.; Logunov, I.; Sheves, M.; Xu, D. Isr J Chem 1995, 35, 447; Ben-Nun, M.; Martinez, T. J.; Molnar, F.; Lu, H.; Phillips, J. C.; Schulten, K. Faraday Disc 1998, 110, 447; Humphrey, W.; Lu, H.; Logunov, I.; Werner, H. J.; Schulten, K. BioPhys J 1998, 75, 1689.
11. Garavelli, M.; Celani, P.; Bernardi, F.; Robb, M. A.; Olivucci, M. J Am Chem Soc 1997, 119, 6891; Vreven, T.; Bernardi, F.; Garavelli, M.; Olivucci, M.; Robb, M. A.; Schlegel, H. B. J Am Chem Soc 1997, 119, 12687; Garavelli, M.; Vreven, T.; Celani, P.; Bernardi, F.; Robb, M. A.; Olivucci, M. J Am Chem Soc 1998, 120, 1285.
12. Car, R.; Parrinello, M. Phys Rev Lett 1985, 55, 2471.
13. Gibson, D. A.; Ionova, I. V.; Carter, E. A. Chem Phys Lett 1995, 240, 261; Liu, Z.; Carter, L. E.; Carter, E. A. J Phys Chem 1995, 99, 4355; Gibson, D. A.; Carter, E. A. Chem Phys Lett 1997, 271, 266; da Silva, A. J. R.; Cheng, H.-Y.; Gibson, D. A.; Sorge, K. L.; Liu, Z.; Carter, E. A. Spectrochim Acta 1997, A53, 1285.
14. Frisch, M. J.; Trucks, G. W.; Schlegel, H. B.; Gill, P. M. W.; Johnson, B. G.; Robb, M. A.; Cheesemann, J. R.; Keith, T.; Petersson, G. A.; Montgomery, A.; Raghavachari, K.; Al-Laham, M. A.; Zakrzewski, V. G.; Ortiz, J. V.; Foresman, J. B.; Peng, C. Y.; Ayala, P. Y.; Chen, W.; Wong, M. W.; Andres, J. L.; Replogle, E. S.; Gomperts, R.; Martin, R. L.; Fox, D. J.; Binkley, J. S.; Defrees, D. J.; Baker, J.; Stewart, J. J. P.; Head-Gordon, M.; Gonzalez, C.; Pople, J. A. GAUSSIAN 94; E1, E2 Gaussian Inc.: Pittsburgh, PA, 1995.
15. Swope, W. C.; Andersen, H. C.; Berens, P. H.; Wilson, K. R. J Chem Phys 1982, 76, 637.
16. Andersen, H. C. J Comput Phys 1983, 52, 24.